Intraurban Temperature Variability in Baltimore

ANNA A. SCOTT, BEN ZAITCHIK, AND DARRYN W. WAUGH

Department of Earth and Planetary Sciences, The Johns Hopkins University, Baltimore, Maryland

KATIE O'MEARA

Architectural Design Department, Maryland Institute College of Art, Baltimore, Maryland

(Manuscript received 24 June 2016, in final form 3 October 2016)

ABSTRACT

How much does minimum daily air temperature vary within neighborhoods exhibiting high land surface temperature (LST), and does this variability affect agreement with the nearest weather station? To answer these questions, a low-cost sensor network of 135 "iButton" thermometers was deployed for summer 2015 in Baltimore, Maryland (a midsized American city with a temperate climate), focusing on an underserved area that exhibits high LST from satellite imagery. The sensors were evaluated against commercial and NOAA/NWS stations and showed good agreement for daily minimum temperatures. Variability within the study site was small: mean minimum daily temperatures have a spatial standard deviation of 0.9°C, much smaller than the same measure for satellite-derived LST. The sensor-measured temperatures agree well with the NWS weather station in downtown Baltimore, with a mean difference for all measurements in time and space of 0.00°C; this agreement with the station is not found to be correlated with any meteorological variables with the exception of radiation. Surface properties are found to be important in determining spatial variability: vegetated or green spaces are observed to be 0.5°C cooler than areas dominated by impervious surfaces, and the presence of green space is found to be a more significant predictor of temperature than surface properties such as elevation. Other surface properties—albedo, tree-canopy cover, and distance to the nearest park—are not found to correlate significantly with air temperatures.

1. Introduction

Extreme temperature is now the deadliest form of climate hazard worldwide (WMO 2014), and heat waves—extended periods of elevated heat and humidity—are a growing problem in most of the United States (IPCC 2013). The health impacts of heat waves are potentially exacerbated by growing urban populations as well as the urban heat island (UHI) effect, a land–atmosphere interaction that causes cities to be several degrees hotter than rural areas. The effect is most pronounced at night and thus is understood to be caused by urban–rural differences in cooling rates (Oke 1982). Temperature differences between cities and rural surroundings have been measured around the world (Oke 1982). These measurements have typically been taken assuming an idealized city with a densely populated, highly urbanized core surrounded by more vegetated and sparsely populated suburbs. Correspondingly, temperature is schematized as decreasing with radial distance from the dense urban core.

Less well quantified is variability within the UHI (Arnfield 2003), which in some cases has been documented to be as large as the urban–rural difference or enough to offset it (Jonsson 2004). A number of recent studies have started closing this gap through installing in situ monitoring networks (e.g., Chapman et al. 2015; Schatz and Kucharik 2014; Mikami et al. 2003; Smoliak et al. 2015) or using private networks [e.g., Hardin (2015) analyzes data from the National Oceanic and Atmospheric Administration (NOAA) and the Earth Networks, Inc., UrbaNet]. These networks are not yet widespread [for a recent list of such networks, refer to Schatz and Kucharik (2014)], however, and their focus on urban–rural differences smooths over neighborhood- and subneighborhood-level variability that may be of interest to urban planners. Many cities have an urban weather station with data that are available to researchers and decision-makers. The term "urban" describes a wide range of characteristics in the built and natural environment, and so urban stations may be located

Corresponding author e-mail: Anna A. Scott, annascott@jhu.edu

DOI: 10.1175/JAMC-D-16-0232.1

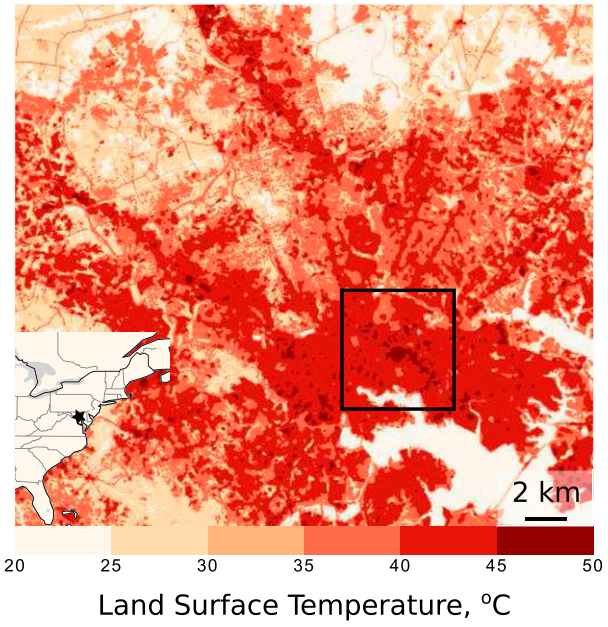

FIG. 1. A thermal LST map of Baltimore from *Landsat-8* (Land Processes Distributed Active Archive Center product obtained online at https://earthexplorer.usgs.gov/) from July 2015. The boxed inset surrounds the neighborhoods of focus in this study.

in areas that differ markedly enough in characteristics from residential neighborhoods to affect their temperature readings by up to several degrees (Stewart and Oke 2012). Understanding how temperatures may differ from a centrally monitored temperature is critically important to health professionals and urban planners, who may rely on central stations to assess the health burden of heat, issue local heat-related weather alerts and closures, or target UHI mitigation strategies.

One way to assess spatial variability within the UHI is through satellite-derived land surface temperature (LST). Some progress has been made developing algorithms to derive air temperature from LST (Ho et al. 2014; Sun et al. 2005; Kloog et al. 2014), but this is not yet widespread, and numerous UHI studies use LST (e.g., Zhao et al. 2014; Nichol et al. 2009; Xu and Liu 2015; Ho et al. 2016; White-Newsome et al. 2013). Although LST is not equivalent to the 2-m air temperature of concern to human comfort, a number of studies show a relationship between the surface UHI and the UHI as measured by air temperature (Voogt and Oke 2003; Arnfield 2003; Nichol and To 2012), and living in an area with high LSTs has been associated with higher mortality during periods of high heat (Smargiassi et al. 2009; Laaidi et al. 2012; Harlan et al. 2013; Hondula et al. 2012).

We aim to ask, how much does minimum daily air temperature vary within neighborhoods exhibiting high LST, and does this variability affect agreement with the nearest weather station? We address these questions using measurements from Baltimore, Maryland, a mid-sized American city on Chesapeake Bay. Satellite-derived LSTs show spatial variability within Baltimore, including the tendency for downtown areas to be warmer than tree-lined areas on the urban periphery (Fig. 1). Satellite measurements show that the hottest neighborhoods are characterized by little vegetation, few trees, and impervious surfaces; they are also the most underserved economically (Huang et al. 2011). In such locations, satellite LSTs can exceed those of downtown by 5°–10°C. Baltimore experiences hot, humid summers and has a Köppen–Geiger climate classification of Cfa, indicating a warm temperate climate, year-round humidity and precipitation, and hot summers (Peel et al. 2007). Accordingly, the Baltimore city government considers heat-stress management to be a top priority for disaster preparedness and climate change adaptation (Baltimore Office of Sustainability 2013). The boxed area in Fig. 1 is the target of city interventions to reduce energy use and potentially temper the UHI through urban greening initiatives. Specifically planned are planting additional street trees, creating pocket parks, focusing community outreach and education efforts, and installing so-called cool roofs (roofs made with highly reflective paint or other covering) in the target neighborhoods. A number of studies circumstantially support the use of urban greening to cool an urban area; most of them use models or satellite data to fill in the sporadic station availability that is common to most urban areas (Bowler et al. 2010). A number of studies from past decades have examined the effects of urbanization on urban heating as cities have grown—notable are studies in Columbia, Maryland (Landsberg 1979), and Phoenix, Arizona (Balling and Brazel 1987), but it is exceedingly rare to have the chance to study urban modifications as they are implemented. Critical to this is a baseline understanding of urban temperature variability at the subneighborhood scale before any changes are implemented.

This paper presents results from a dense, low-cost air temperature sensor network in Baltimore (Fig. 1) in an unprecedented characterization of air temperature at subneighborhood resolution. This network is part of a larger interdisciplinary UHI project (Zaitchik et al. 2016). Our measurements focus on extensively sampling a thermal hot spot in eastern Baltimore (see boxed inset of Fig. 1) using a network of Maxim Integrated Products, Inc., "iButton" Model DS1923 Hygrochron thermometer/hygrometers and weather stations from the NOAA/National Weather Service (NWS) and the Davis Instruments company. We discuss and validate our temperature sensors in section 2. The spatial variability of the

FIG. 2. Two examples of sensors deployed in trees in an underserved eastern Baltimore neighborhood that is characterized by low tree cover and a large percentage of impervious surfaces as well as by high vacancy rates: (a) a site that typifies a park or green space and was listed as green space and partial shade and (b) a site that is characteristic of an impervious streetscape and was listed as impervious and partial shade.

network and the connection with surface properties are presented in section 3, and some implications for urban policy are discussed in section 4.

2. Materials and methods

a. Observations

Data used in this paper come from an NWS weather station, a Davis Instruments Vantage Pro2 weather station, satellites, and a network of iButtons. The iButtons provide a stand-alone thermometer, hygrometer, and datalogger system that is the size of a standard watch battery and have a reported accuracy of 0.5°C for the temperature ranges that were experienced during the reporting period. This accuracy was confirmed in laboratory conditions by a random sample of 30 of the buttons (not shown). The iButton and a radiation shield were attached with plastic zip ties to trees (90.4%), wooden posts (2.2%), and metal lampposts or street signs (7.4%) and were removed at the end of the summer recording period.

The iButtons cost relatively little (approximately $70 for the iButton) for an out-of-the-box measuring and datalogging solution. Together, they provide a low-profile microweather station that fits in the palm of a hand and may be installed discreetly in neighborhoods with high foot traffic (Fig. 2). Having a discreet sensor allowed us (the authors) to quickly expand the range of monitoring locations beyond our own neighborhoods and social networks.

We began installing the network of iButtons in June of 2015 and left them to record hourly temperature through mid-September (Fig. 3). More iButtons were added throughout the summer to refine measurements, for a total of 153 iButtons. One round of data collection occurred during mid-July. By the time of sensor collection in October, 135 remained. Results were checked for different time periods and were found to be insensitive to the period of data analysis: changes in the sensor network did not affect our conclusions. Data collection focused on eastern Baltimore neighborhoods; sensors were placed approximately 150 m apart on five transects,

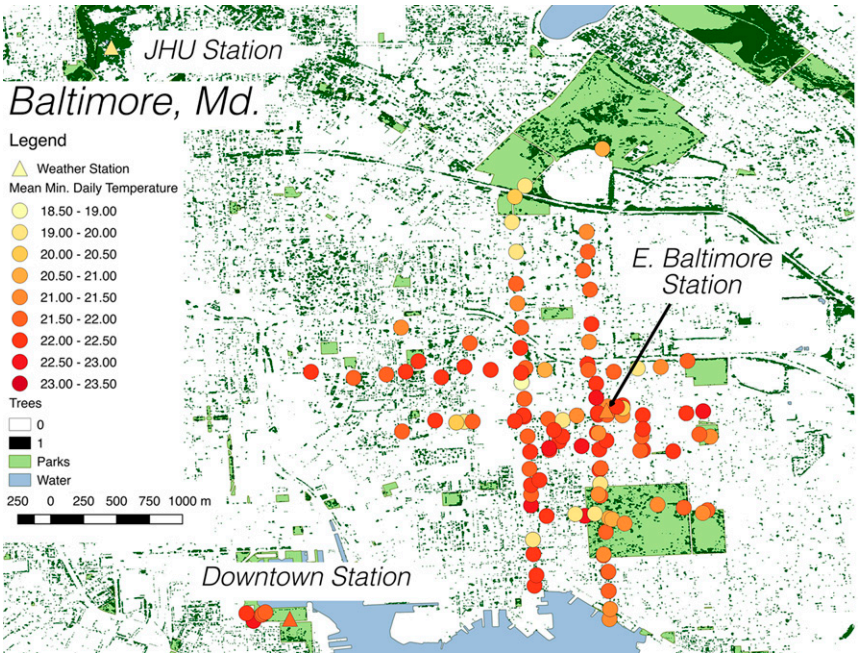

FIG. 3. Locations of the 135 sensors in eastern Baltimore. The color scale shows $\overline{T}$, the temporal mean of daily minimum temperatures for 1 Jun–15 Sep 2015.

of which three were east–west and two were north–south, ranging from 1.6 to 4 km long. Additional iButtons were installed in neighborhood parks and near weather stations for data validation. Most of the landscapes in this area are homogeneous. Two- or three-story brick row houses are the main housing stock (Fig. 2b), corresponding to local climate zone (LCZ) 3, that is, the compact low-rise LCZ (Stewart and Oke 2012). Much of the landscape variability comes from the presence of trees (LCZ B: scattered trees) or grass and vegetation (LCZ D: low plants), as seen in Fig. 2a, although the center of the transects passes through a four-block-by-four-block urbanized zone (LCZ 1: the compact high-rise LCZ) that is home to the Johns Hopkins Medical Campus.

Each iButton was installed facing north. At each installation location, scientists 1) recorded the land cover as impervious, grass, or soil, 2) recorded the installation site (trees, metal poles, or wood posts), and 3) estimated the amount of shade as full shade, partial shade, or none (i.e., full sun). Land cover takes into account the ambient conditions as opposed to the purely local conditions. For example, a tree sitting in a tree well with exposed soil is listed as impervious if the surrounding area is concrete or asphalt, and a sensor in a vegetated but vacant lot is specified as being in a green space even if the sensor is not located in a park or in an official city green space. Shade measurements, by comparison, are purely local and only take into account the estimated amount of sunlight that the sensors receive. Figure 2 illustrates typical sites that were both listed as partial shade; 5.9% of sensors were in full sun, 45.2% were in partial shade, and 48.9% were in full shade.

As noted in Chapman et al. (2015) and WMO (2010), urban air temperature sampling comes with unique challenges. Standard meteorological siting protocols are often inapplicable in urban areas, and it was particularly challenging to find any locations for sensor installation that reflect the average ambient conditions in many of the neighborhoods studied in this paper. For example, trees are thought to be a source of urban cooling (Kleerekoper et al. 2012), but our sampling method relies on the presence of at least a few trees. A majority of the iButtons were installed on trees (90.4%), but on occasion no trees were available in what would be considered average residential conditions, causing sampling to shift to locations in vacant and vegetated lots or wooded alleyways. This is perhaps one form of sampling bias. In addition, brick row houses dominate the landscape (see Fig. 2) and release heat at night, which may cause street-adjacent readings to differ from those taken farther from buildings. Despite these challenges, we argue that our sampling method reasonably balances the need for rigorous meteorological standards with the need for data in an understudied environment.

In addition to the iButton network, daily temperature data are also available from an NWS weather station located in downtown Baltimore at the Maryland Science

Center, hereinafter referred to as the downtown station (Fig. 3). We used a 15-yr record to calculate an extreme temperature threshold from the 95th percentile of minimum daily temperature. Because the downtown station is only 15 years old, we checked this threshold against a longer period (1975–2014) at the Baltimore–Washington International Airport NWS synoptic station, which is approximately 12 km south-southwest of the study site. The two extreme temperature thresholds were found to be consistent with their mean difference of 2°C. NWS station thermometers are aspirated and have a reported accuracy of 0.56°C (Diamond et al. 2013).

Hourly meteorological data (wind, pressure, relative humidity, and radiation) are also taken from a Davis Instruments Vantage Pro2 weather station installed at The Johns Hopkins University on the roof of Olin Hall (referred to as the JHU station). A similar station was installed during midsummer in eastern Baltimore at 2-m height in the greened interior of a residential block; the wind and radiation data from the JHU station were checked against these data and were found not to differ significantly. For continuity, only the JHU station data were used. The Vantage Pro2 has a reported accuracy of 0.5°C for the temperature ranges seen during the reporting period and is naturally aspirated.

A number of satellite-derived observations are also used. The *Landsat-8* (Land Processes Distributed Active Archive Center product obtained online at https://earthexplorer.usgs.gov/) image from 1046 local time 16 July 2015, which is the least cloudy image available for the observation period, was used to calculate both LST and albedo. Nighttime Landsat scenes are not available for this period. To derive LST, band-10 digital-number data are converted to top-of-atmosphere at-sensor radiance and then at-satellite brightness temperature following the method of Jiménez-Muñoz and Sobrino (2003). To account for the different surface emissivities, we use the U.S. Geological Survey (USGS) land-cover map to categorize the brightness temperatures by land type and assign them an emissivity value, as in Alipour et al. (2010). We then apply a correction for atmospheric water vapor to the brightness temperature following the monowindow algorithm in Qin et al. (2001). Climatological temperature from the weather station at The Johns Hopkins University is used to determine the surface air temperature, which is then used to estimate atmospheric temperature aloft.

The *Landsat-8* scene was also used to calculate albedo using a normalized form of the Liang (2001) approach as outlined in Smith (2010). Satellite-derived tree-canopy data at 10-ft (305 cm) resolution (Fig. 3) were provided by TreeBaltimore (http://treebaltimore.org/). Elevation data come from the Maryland lidar dataset for the city of Baltimore (http://lidar.salisbury.edu/arcgis/rest/services/ShadedRelief/MD_baltimorecity_shadedRelief_RGB/ImageServer), and the park shapefile data were downloaded from Baltimore OpenData (https://data.baltimorecity.gov/).

b. *Measurement evaluation*

iButtons come precalibrated for laboratory settings, but meteorological air temperature must be measured in the shade (WMO 2010). Shielding is then the principal source of error for outdoor temperature measurements, although poor aspiration or siting thermometers near sources of heat can also contribute to error. The iButtons and shield used in this study were evaluated against a Vantage Pro2 naturally aspirated weather station and an aspirated NWS station. The results, shown in Fig. 4, indicate that sensors agree well with station data for minimum daily temperatures. Diurnal results indicate that the sensors agree at night but that significant differences are detected during daytime hours (2°C or more). Because the daytime differences between the iButton and station temperatures were not well correlated with humidity, wind speed, or incoming solar radiation, they are omitted from this analysis. Microclimatic differences may be exaggerated during the day, but we argue that a focus on daily minimum temperatures makes sense in the context of the UHI, a phenomenon that is maximized at night and largely disappears during the daytime. The greatest need for local data is then at night and in the early morning; therefore, temperatures were collected hourly for the period from 1 June to 15 September 2015 and were subsampled to obtain $T = T_{\min}(x_i, t)$, which is a time series of daily minimum temperatures at each sample location x_i. This dataset (Scott et al. 2016) is available for download through the Johns Hopkins Data Archive (https://archive.data.jhu.edu/dvn/). Minimum daily temperatures occur at approximately 0600 local time, at which time the mean wind speed is 0.37 m s^{-1} and the mode of the wind direction is north-northeast, although minimum temperatures may not occur simultaneously at each location.

3. Results

The spatial variability of minimum daily air temperatures measured in eastern Baltimore is smaller than expected. For the summertime (temporal) mean of daily minimum temperatures seen in Fig. 3, the standard deviation is 0.9°C, which is small relative to the seasonal range of 20°C and small even in the context of the range of temporal mean temperatures, 4.15°C. The distribution of all observed air temperatures is nearly normal (Fig. 5a), with a temporal–spatial mean temperature $\langle \overline{\Delta T} \rangle$ = 21.7°C. Here, $\langle T \rangle$ refers to spatially averaged temperature and $\overline{T}$ refers to temporally averaged

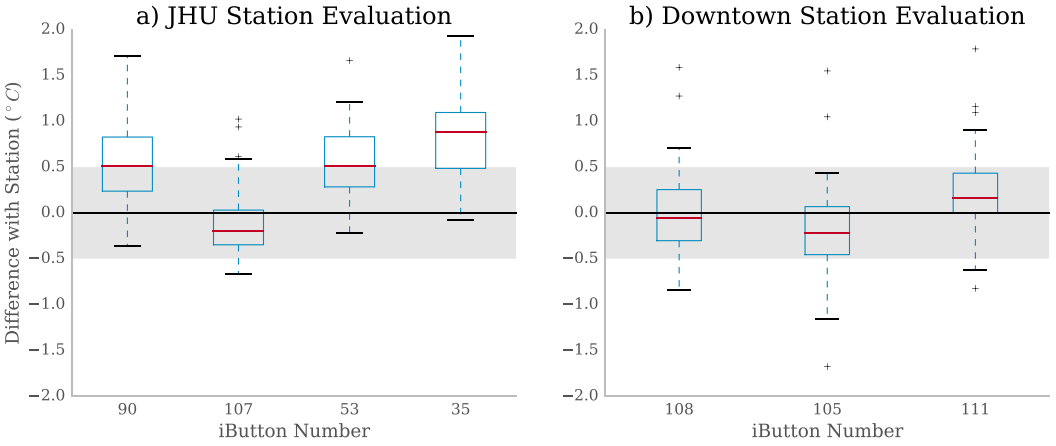

FIG. 4. A summary of the difference between selected iButtons and weather stations located (a) at JHU and (b) downtown. Each column represents the distribution of 68 measurements from one iButton sensor minus the station for daily minimum temperature for 10 Jul–15 Sep 2015. Red lines represent the median of the data, the blue box represents the interquartile range, (IQR = [Q1, Q3], where Q1 is the 25th percentile and Q3 is the 75th percentile), and black lines represent the wide interquartile range ([Q1 − 1.5 × IQR, Q3 + 1.5 × IQR]). Outliers outside this range are shown with plus signs; for the JHU station evaluation, one outlier from each column ranging from 5° to 6°C is omitted. The shaded area is the accuracy of the iButton (±0.5°C).

temperature. This value was calculated by averaging first over time at each sensor and then over space.

The distribution of temperature (Fig. 5a) measured at the downtown station is similar to the distribution of temperatures in eastern Baltimore. The mean and range of eastern Baltimore and the downtown station are also similar, and when eastern Baltimore and station data are plotted as a time series (Fig. 5b), very little difference is discernible. The summer of 2015 experienced several periods of extreme heat, seen where the station temperature exceeds the extreme heat threshold, as well as cooler periods (Fig. 5b); this day-to-day meteorological variability contributes to the wide range of temperatures seen in the histograms and explains why the reported standard deviation of temporal mean temperatures, 0.9°C, is much smaller than the standard deviation of all data, 2.78°C. The distribution of temperature differences with the downtown station, $\Delta T(x_i, t) = T_i - T_{\text{downtown}}$, is nearly normal (Fig. 5c) and has a low standard deviation ($\sigma = 1.37$); these statistics were computed by equally weighting each measurement in space and time. The mean difference $\overline{\Delta T(x_i, t)} \approx 0.00$°C is negligible and is much less than the precision of either the iButton or downtown station thermometer. Because nearly all of the data fall within ±2°C, we conclude that the downtown Baltimore station is a reasonable way to assess average thermal conditions in eastern Baltimore.

Mean agreement with the weather station does not appear to vary with weather conditions. This was assessed by correlating meteorological variables with the spatial mean temperature difference with the downtown station $\langle \Delta T \rangle(t) = \langle T_i - T_{\text{downtown}} \rangle$ (Figs. 6a,c,e,g). Meteorological variables are calculated as the mean of the previous day (i.e., lagged 1 day), and the correlation coefficient r is calculated as the Pearson product-moment correlation coefficient. The observation period covered several periods of extreme heat (Fig. 5b), but the correlation between the previous day's temperature and spatially averaged daily $\langle \Delta T \rangle$ is insignificant ($r = 0.003r = 0.003$, with two-tailed p value of 0.98; Fig. 6a), indicating that periods of extreme heat do not affect agreement with the downtown station. Increased wind speed, pressure, and radiation all had insignificant correlations with temperature difference (Figs. 6c,e,g). The insignificance of these correlation values leads us to conclude that mean sensor agreement is not explained by meteorological conditions.

In addition, much of the variability in observed air temperature in Fig. 5 is due to temporal variability rather than to spatial variability. First, the downtown station and the sensor network have the same standard deviation ($\sigma = 2.8$; Fig. 5a). When the data are time averaged and this meteorological variability is removed, the standard deviation falls from 2.78° to 0.9°C. Second, sensor-to-sensor agreement with the downtown station does not correlate significantly with meteorological variables except for radiation (Figs. 6b,d,f,h). This was assessed by correlating meteorological variables with $\sigma\Delta T = \sigma[T(x_i) - T_{\text{downtown}}]$, the time-varying spatial standard deviation of agreement with the station. This measure assesses the sensor-to-sensor variability in station agreement or, more broadly, temperature

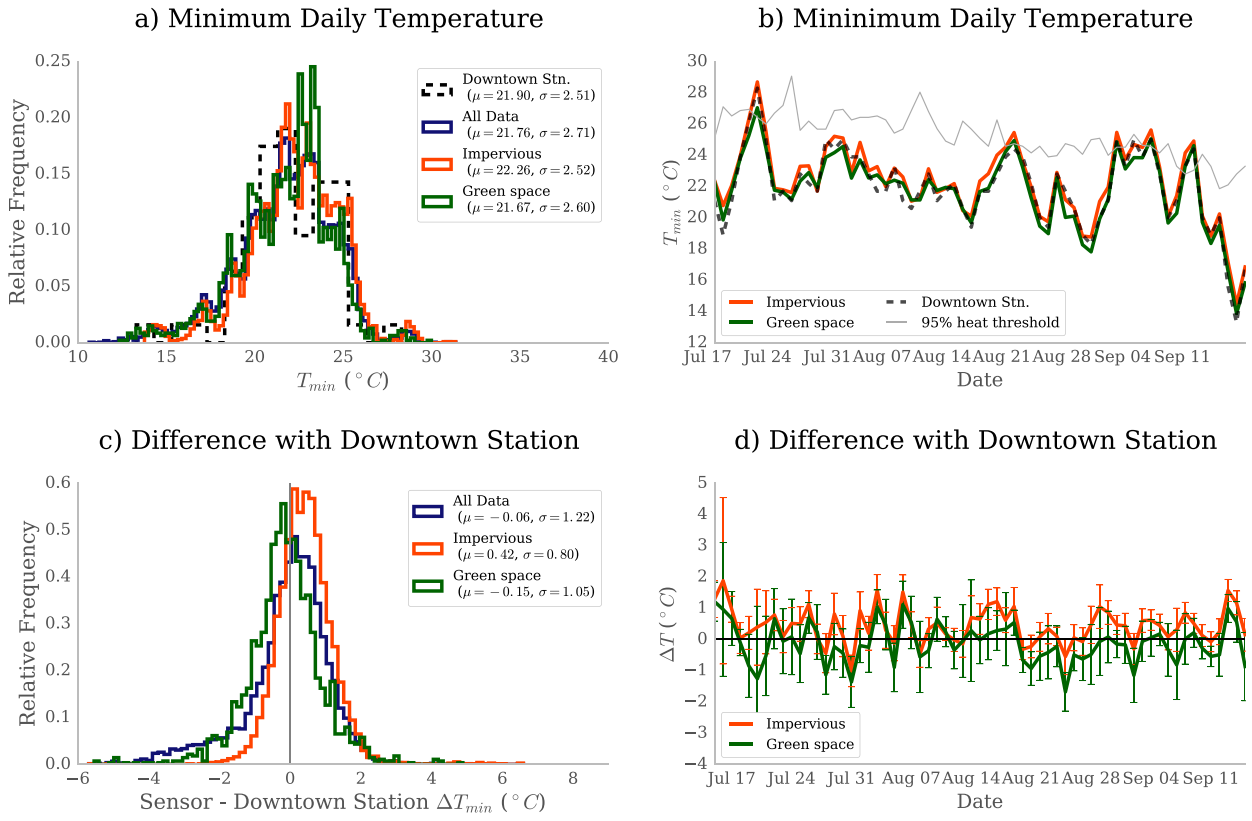

FIG. 5. (left) Histogram and (right) time series of (a),(b) the eastern Baltimore temperature data and (c),(d) the difference with the downtown station for daily minimum temperature for sensors. The station data count in (a) is inflated by a factor of 100 to appear on the same scale as the iButton data. Green and orange lines represent sensors located in green spaces and impervious spaces, respectively. An extreme temperature threshold is shown in (b) (light gray) and represents the 95th percentile of temperature for 2000–15. Difference with the downtown station in (c) is calculated as $\Delta T = T_i - T_{\text{downtown}}$ and is spatially averaged in (d) to compute $\langle \Delta T(t) \rangle = \langle T_i - T_{\text{downtown}} \rangle$ for $i \in \{\text{impervious, green space}\}$. Error bars in (d) give the spatial standard deviation, representing sensor-to-sensor variability.

variability in the spatial sense. There are insignificant correlations ($|r| < 0.1$, with $p > 0.2$) with mean temperature, wind speed, and pressure. The correlation of radiation with temperature variability (Fig. 6h; $r| = 0.25$, with $p < 0.05$) is the only significant correlation and shows that sunnier conditions increase the chance that a given sensor may disagree with the downtown station. We note, however, that the variability is still small, with a range of 1°C or so.

The spatial variability of eastern Baltimore air temperature is also much less than what is suggested by daytime LST in Fig. 1. Satellite-derived urban–rural differences are largest during the day, whereas the air temperature differences are largest at night, and therefore, even though minimum daily T_{air} and daytime satellite temperature measurements do not occur at the same time, the two are comparable in the sense that both may be used to assess the UHI intensity. As expected, the mean of minimum daily air temperatures is much lower than that of LST: $\langle \overline{T} \rangle = 21.1$°C as compared with $\langle \text{LST} \rangle = 43.3$°C, respectively. The standard deviation σ and range R of air temperature are also lower than those of LST: $\sigma(\overline{T}) = 0.9$°C as compared with $\sigma(\text{LST}) = 2.07$°C and $R(\overline{T}) = 4.15$°C versus $R(\text{LST}) = 7.9$°C. The discrepancy between air temperature and LST in the mean, variability, and range shows the potential caveats of using LST and air temperature interchangeably to diagnose the severity of urban heating.

Much of the sensor-to-sensor spatial variability can then be explained by variability in land cover and in particular whether a sensor is placed in an area dominated by impervious or green space. Green spaces, or spaces dominated by grass and other vegetation, are cooler than impervious spaces on average by 0.56°C (Fig. 5a). Although small, the difference is found to be significant by a Welch's t test [p value of 1.9×10^{-10} using the "SciPy" (https://www.scipy.org/) Python library's "stats.ttest_ind" function]. This difference explains 12% of the variability in mean minimum daily temperature. Green spaces are also on average cooler

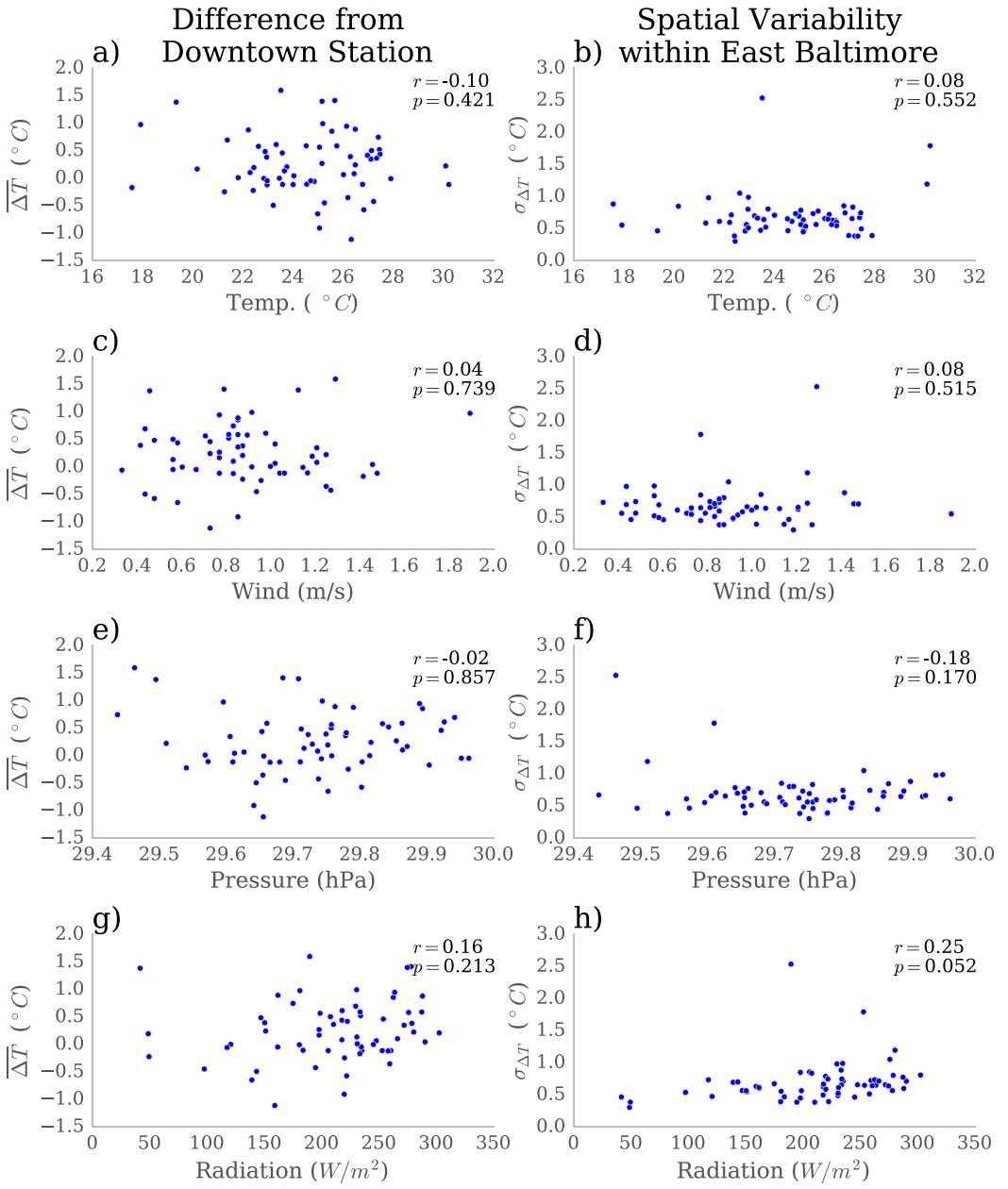

FIG. 6. The relationship between meteorological conditions and the downtown station. (a),(c),(e),(g) The relationship between meteorological variables and temperature differences $\overline{\Delta T} = \langle T_{\text{sensor}} - T_{\text{downtown}} \rangle$. (b),(d),(f),(h) The relationship between meteorological variables and spatial variability within eastern Baltimore as shown by $\sigma\Delta T = \sigma(T_{\text{sensor}} - T_{\text{downtown}})$, the spatial standard deviation of agreement with the downtown station. Meteorological variables come from the JHU station; shown are daily averages lagged by 1 day. The correlation coefficient r is calculated as the Pearson product-moment correlation coefficient.

than the downtown station, whereas impervious spaces are slightly warmer, although this difference is slight: $\langle \Delta T \rangle_{\text{green}} = -0.18$°C versus $\langle \Delta T \rangle_{\text{impervious}} = +0.39$°C. Because meteorological standards encourage siting weather stations around fields and vegetated areas (WMO 2014), it is important to note that microclimate effects may influence temperature when using standard weather station data to assess local urban conditions, even at night.

Nighttime temperatures correlate insignificantly with other surface properties (Fig. 7), with the exception of elevation. The relationship between surface properties and temperature was assessed by correlating elevation, albedo, a sensor's distance from an official park, and the

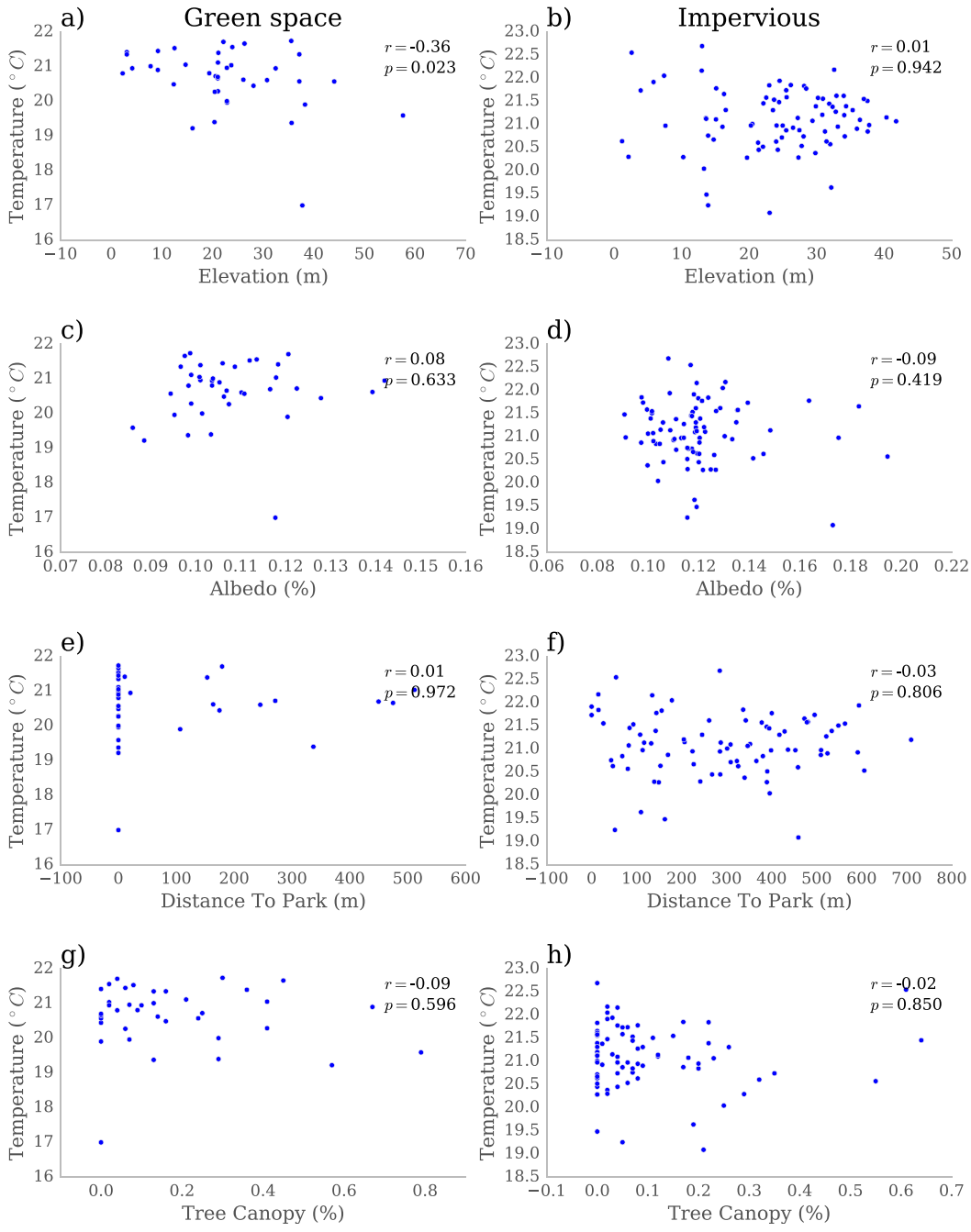

FIG. 7. The relationship between $\overline{T}$ and surface properties at each sensor located in (a,)(c),(e),(g) green spaces and (b),(d),(f),(h) impervious spaces; also given is the Pearson product-moment correlation coefficient r.

calculated percent tree-canopy cover for a 33-m^2 box centered around the sensor with time-averaged $\overline{T}$. For green spaces, only elevation correlates significantly with $\overline{T}$. Tree canopy, elevation, and albedo correlate insignificantly. None of the examined surface variables correlate significantly with temperatures taken in impervious spaces. The insignificant correlations with park distance may be affected by using the official inventory of park locations—the Baltimore city government runs an adopt-a-lot program that allows citizens and community groups to manage vacant lots as parks, gardens, or green spaces without formal recognition and therefore many of the sensors that were counted in green space were not in official parks, especially in neighborhoods

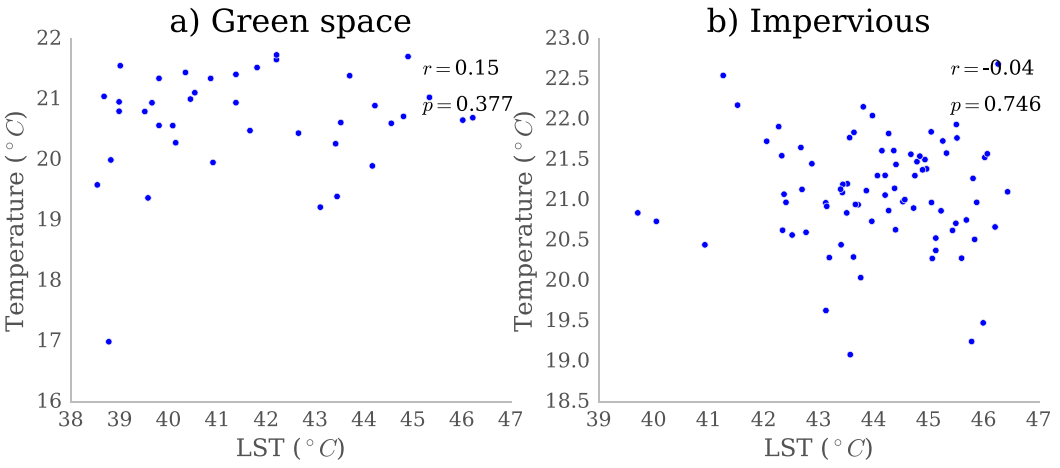

FIG. 8. The relationship between $\overline{T}$ and LST (*Landsat-8*) at each sensor located in (a) green spaces and (b) impervious spaces; also given is the Pearson product-moment correlation coefficient *r*.

where there are fewer parks. This suggests that the larger parks did not have an impact on temperature outside their boundaries. Air temperature is also not correlated significantly with LST (Fig. 8), with $p > 0.75$ for both green and impervious spaces. Although LST is not a surface property, because it changes over time, it is highly correlated with static surface properties such as distance to park ($r = 0.6$). LST and air temperature are both used as measures to diagnose urban heating, and therefore it is notable that on the neighborhood scale the correlation is so poor.

Regression analysis confirms that the presence of green space is a predictor of mean air temperature and is the only reliable predictor of the aspects examined (LST, albedo, distance to park, and tree-canopy cover). Ordinary least squares regression with elevation and presence of green space (1 for green space; 0 for impervious) against mean daily minimum temperature gives the following result:

$$\overline{T} = 21.3 - 0.01x_{\text{elevation}} - 0.51x_{\text{greenspace}},$$

which explains 11% of the variability ($r^2 = 0.11$). Elevation is included because it correlated strongly with green-space temperature ($r = -0.36$) and because green space occurs at a range of elevations (0–60 m). Only presence of green space is statistically significant at the 95% confidence level ($p = 0.000$ for green space; $p = 0.11$ for elevation). Other tested variables were collinear, for example, albedo and tree cover, and so could not produce a robust regression result. The regression coefficient for $x_{\text{greenspace}}$ indicates that, after controlling for elevation, temperatures decrease by 0.5°C when entering a green space. This is more than the mean difference of 0.6°C between impervious and green space indicated in Fig. 5a; because green space is more abundant at lower elevations (Fig. 7a), this result suggests that elevation is masking some of the cooling effects of parks and green spaces.

4. Discussion

Although previous studies have shown that parks are approximately 1°C cooler during the day (Bowler et al. 2010), it was unexpected that green spaces would be cooler at night. Although during the day release of latent heat by parks and vegetated areas is probably the source of cooling, at night condensation could cause warming. To explain this, we can offer some hypotheses, although an analysis of the mechanisms for urban cooling are beyond the scope of this paper. If one takes the approach of Oke et al. (1991), the net energy budget of the urban surface can be understood to be $L + S + R = Q_{\text{net}}$, where L represents latent heat flux, S represents sensible heat flux, R is the radiative heat flux, and Q_{net} is the residual flux, which is nonzero throughout the course of the day. Because wind speed during the nighttime hours is low, sensible heat is low; enhanced radiative cooling could explain why parks are efficient at nighttime cooling. This is further influenced by differing material properties, such as thermal capacity, conductance, and emissivity. Geometry—in particular, the sky-view factor—may also play a role because parks tend to be more open and thus have greater radiative loss. We do not presently see a relationship between park size and temperature, but this is limited by the study area and number of parks present in this study, and so we cannot generalize. Perhaps a larger-scale study could find such a connection.

Our conclusion that wind speed, as measured at weather stations, appears to be less important than surface properties is interesting in light of a recent UHI study in Birmingham, United Kingdom, in which wind speed and direction were found to play an important role in governing urban heating (Azevedo et al. 2016). Although a number of studies in the literature have found that low wind speeds would allow for more temperature heterogeneity within the UHI (e.g., Oke 1982; Schatz and Kucharik 2014), our study found insignificant relationships between daily wind speed and temperature differences with the station. This result suggests that any changes associated with increasing wind speed are experienced uniformly within the study area.

As the climate warms, more cities seek cost-effective strategies to cool their neighborhoods, such as greening plans that increase the amount of vegetated surfaces and increase tree canopy (e.g., Kleerekoper et al. 2012). Although this paper is not intended to evaluate these strategies, our findings do suggest some possible limitations to interventions implemented at the neighborhood scale, especially for the levels of vegetation found in eastern Baltimore. Our analysis does find that vegetated spaces are significantly cooler than impervious spaces, but this effect is found to be small and very localized: only 0.5°C, even after controlling for the effects of elevation. This is not sufficient to offset urban heating, which is often several degrees or more. One possible policy intervention supported by this work is local greening near where residents are likely to congregate, such as planting more and smaller parks or grass sidewalk right-of-ways in residential areas. At this time, our results would support greening policies that begin with planting grass or other low vegetation rather than tree planting. We caution that the low tree-canopy-cover amounts that were present in our study area (most locations had tree-canopy coverage of 0%–30%) may prevent drawing conclusions about the potential of increasing tree canopy, because the overall tree canopy in this neighborhood is low. Although these ranges of tree canopy were not found to be sufficient to cool impervious surfaces, there may still be a threshold level above which this is not true.

We also caution that differing climate zones and city landscapes may prevent the results of this study from being directly applied to other areas. One lesson we think will apply to other cities is how geospatial relationships with surface properties may change according to scale; findings that apply at the citywide scale may not be relevant at the neighborhood and subneighborhood level. This has the possibility to complicate possible policy interventions. We found this to be true for relationships between air temperature and LST: we found that the point-to-point correlation between LST and air temperature was poorer than what was indicated in the literature. Such studies looked at this relationship on larger scales, however (e.g., Kloog et al. 2014; Nichol and To 2012; Nichol et al. 2009). This conclusion agrees with White-Newsome et al. (2013), who found a poor correlation between LST and air temperature when comparing point to point but had better results when averaging LST at radii of larger than 200 m. This may also be true for other variables, such as tree-canopy cover or albedo.

5. Conclusions

Summertime air temperature measurements in Baltimore using 135 low-cost air temperature sensors show that much of the spatial variability in daily minimum air temperature is small and that some of this variability (11%) is explained by surface properties, namely, the presence or absence of vegetation, and is not well explained by meteorological conditions. The time-averaged minimum daily temperatures have a spatial standard deviation (0.9°C) that is much smaller than the same measure for satellite-derived LST (2.07°C), and the sensor-measured temperatures agree well with the NWS weather station in downtown Baltimore, with a mean difference for all measurements in time and space of 0.00°C. The presence or absence of vegetation affected temperature more than did other meteorological and surface properties examined, and time-averaged air temperatures in green spaces are found to be cooler than impervious spaces by approximately 0.5°C.

This work suggests that using thermal satellite imagery to estimate the variability of minimum daily air temperatures will exaggerate air temperature variability and that care must be taken when using thermal imagery in place of in situ air temperature measurements to diagnose urban heating. Because the mean differences with the downtown weather station are not statistically significant, these findings support the use of the downtown weather station in Baltimore to assess average thermal conditions, even in thermally identified hot spots.

This work raises a number of questions. As discussed above, an open question is why green spaces are cooler at night. Another question is whether our findings will hold up when examined on a citywide basis. More work is ongoing to answer this latter question, and it is hoped that the work will help to answer questions about how densely temperature must be monitored to capture the subneighborhood variability of interest to our partners in public health and urban planning. This study examined areas that were largely homogeneous in terms of the built environment; for a geographically expanded

study, pairing data with a standard measure of urbanization or classification such as a brightness index or the local climate zone classification could help comparisons with ongoing work in other cities.

Acknowledgments. We acknowledge Kristin Baja and the Baltimore City Department of Sustainability, National Science Foundation (NSF) IGERT Grant DGE-1069213, NSF Hazards SEES Grant 1331399, and the Johns Hopkins Department of Earth and Planetary Science summer field fund for their support, as well as Clara Hickman, Sophie Stoerkel, and the Maryland Institute College of Art for the radiation shield design. We also thank Erik Jorgensen, Jasmin Gonzalez, Dillon Ponzo, and Celine Sze for their invaluable help with fieldwork, as well as Emma Eklund for her work on satellite data. Our community partners helped greatly with community outreach and helped guide our installation process; in particular, we thank Beth Meyers-Edwards and Banner Neighborhoods, as well as Jennifer Kunze and the Amazing Grace Evangelical Lutheran Church.

REFERENCES

Alipour, T., M. R. Sarajian, and A. Esmaeily, 2010: Land surface temprature [sic] estimation from thermal band of Landsat sensor, case study: Alashtar city. *Int. Arch. Photogramm. Remote Sens. Spat. Inf. Sci*, **38-4/C7**, 6 pp. [Available online at https://www.researchgate.net/publication/215444122_Land_Surface_Temprature_Estimation_Base_on_Thermal_Band_of_ETMSensor.]

Arnfield, A. J., 2003: Two decades of urban climate research: A review of turbulence, exchanges of energy and water, and the urban heat island. *Int. J. Climatol.*, **23**, 1–26, doi:10.1002/joc.859.

Azevedo, J. A., L. Chapman, and C. L. Muller, 2016: Quantifying the daytime and night-time urban heat island in Birmingham, UK: A comparison of satellite derived land surface temperature and high resolution air temperature observations. *Remote Sens.*, **8**, 153, doi:10.3390/rs8020153.

Balling, R. C., Jr., and S. W. Brazel, 1987: Time and space characteristics of the Phoenix urban heat island. *J. Ariz.-Nev. Acad. Sci.*, **21**, 75–81.

Baltimore Office of Sustainability, 2013: City of Baltimore disaster preparedness and planning project. Baltimore City Planning Commission Rep., 179 pp. [Available online at http://www.baltimoresustainability.org/plans/disaster-preparedness-plan/.]

Bowler, D. E., L. Buyung-Ali, T. M. Knight, and A. S. Pullin, 2010: Urban greening to cool towns and cities: A systematic review of the empirical evidence. *Landscape Urban Plann.*, **97**, 147–155, doi:10.1016/j.landurbplan.2010.05.006.

Chapman, L., C. L. Muller, D. T. Young, E. L. Warren, C. S. B. Grimmond, X.-M. Cai, and E. J. S. Ferranti, 2015: The Birmingham Urban Climate Laboratory: An open meteorological test bed and challenges of the smart city. *Bull. Amer. Meteor. Soc.*, **96**, 1545–1560, doi:10.1175/BAMS-D-13-00193.1.

Diamond, H. J., and Coauthors, 2013: U.S. Climate Reference Network after one decade of operations: Status and assessment. *Bull. Amer. Meteor. Soc.*, **94**, 485–498, doi:10.1175/BAMS-D-12-00170.1.

Hardin, A. W., 2015: Assessment of urban heat islands during hot weather in the U.S. Northeast and linkages to microscale thermal and radiational properties. M.S. thesis, Dept. of Atmospheric Science, Texas Tech University, 131 pp. [Available online at http://hdl.handle.net/2346/63661.]

Harlan, S. L., J. H. Declet-Barreto, W. L. Stefanov, and D. B. Petitti, 2013: Neighborhood effects on heat deaths: Social and environmental predictors of vulnerability in Maricopa County, Arizona. *Environ. Health Perspect.*, **121**, 197–204, doi:10.1289/ehp.1104625.

Ho, H. C., A. Knudby, P. Sirovyak, Y. Xu, M. Hodul, and S. B. Henderson, 2014: Mapping maximum urban air temperature on hot summer days. *Remote Sens. Environ.*, **154**, 38–45, doi:10.1016/j.rse.2014.08.012.

——, ——, Y. Xu, M. Hodul, and M. Aminipouri, 2016: A comparison of urban heat islands mapped using skin temperature, air temperature, and apparent temperature (humidex), for the greater Vancouver area. *Sci. Total Environ.*, **544**, 929–938, doi:10.1016/j.scitotenv.2015.12.021.

Hondula, D. M., R. E. Davis, M. J. Leisten, M. V. Saha, L. M. Veazey, and C. R. Wegner, 2012: Fine-scale spatial variability of heat-related mortality in Philadelphia County, USA, from 1983–2008: A case-series analysis. *Environ. Health*, **11**, 16, doi:10.1186/1476-069X-11-16.

Huang, G., W. Zhou, and M. L. Cadenasso, 2011: Is everyone hot in the city? Spatial pattern of land surface temperatures, land cover and neighborhood socioeconomic characteristics in Baltimore, MD. *J. Environ. Manage.*, **92**, 1753–1759, doi:10.1016/j.jenvman.2011.02.006.

IPCC, 2013: Summary for policymakers. *Climate Change 2013: The Physical Science Basis*, T. F. Stocker et al., Eds., Cambridge University Press, 1–29.

Jiménez-Muñoz, J. C., and J. A. Sobrino, 2003: A generalized single-channel method for retrieving land surface temperature from remote sensing data. *J. Geophys. Res.*, **108**, 4688, doi:10.1029/2003JD003480.

Jonsson, P., 2004: Vegetation as an urban climate control in the subtropical city of Gaborone, Botswana. *Int. J. Climatol.*, **24**, 1307–1322, doi:10.1002/joc.1064.

Kleerekoper, L., M. van Esch, and T. B. Salcedo, 2012: How to make a city climate-proof, addressing the urban heat island effect. *Resour. Conserv. Recycl.*, **64**, 30–38, doi:10.1016/j.resconrec.2011.06.004.

Kloog, I., F. Nordio, B. A. Coull, and J. Schwartz, 2014: Predicting spatiotemporal mean air temperature using MODIS satellite surface temperature measurements across the northeastern USA. *Remote Sens. Environ.*, **150**, 132–139, doi:10.1016/j.rse.2014.04.024.

Laaidi, K., A. Zeghnoun, B. Dousset, P. Bretin, S. Vandentorren, E. Giraudet, and P. Beaudeau, 2012: The impact of heat islands on mortality in Paris during the August 2003 heat wave. *Environ. Health Perspect.*, **120**, 254–259, doi:10.1289/ehp.1103532.

Landsberg, H. E., 1979: Atmospheric changes in a growing community (the Columbia, Maryland experience). *Urban Ecol.*, **4**, 53–81, doi:10.1016/0304-4009(79)90023-8.

Liang, S., 2001: Narrowband to broadband conversions of land surface albedo I: Algorithms. *Remote Sens. Environ.*, **76**, 213–238, doi:10.1016/S0034-4257(00)00205-4.

Mikami, T., H. Ando, W. Morishima, T. Izumi, and T. Shioda, 2003: A new urban heat island monitoring system in Tokyo. *Proc. Fifth Int. Conf. on Urban Climate*, Łódź, Poland, International

Association for Urban Climate, O.3.5. [Available online at http://meteo.geo.uni.lodz.pl/icuc5/text/O_3_5.pdf.]

Nichol, J. E., and P. H. To, 2012: Temporal characteristics of thermal satellite images for urban heat stress and heat island mapping. *ISPRS J. Photogramm. Remote Sens.*, **74**, 153–162, doi:10.1016/j.isprsjprs.2012.09.007.

——, W. Y. Fung, K.-S. Lam, and M. S. Wong, 2009: Urban heat island diagnosis using ASTER satellite images and 'in situ' air temperature. *Atmos. Res.*, **94**, 276–284, doi:10.1016/j.atmosres.2009.06.011.

Oke, T. R., 1982: The energetic basis of the urban heat island. *Quart. J. Roy. Meteor. Soc.*, **108**, 1–24, doi:10.1002/qj.49710845502.

——, G. T. Johnson, D. G. Steyn, and I. D. Watson, 1991: Simulation of surface urban heat islands under 'ideal' conditions at night part 2: Diagnosis of causation. *Bound.-Layer Meteor.*, **56**, 339–358, doi:10.1007/BF00119211.

Peel, M. C., B. L. Finlayson, and T. A. McMahon, 2007: Updated world map of the Köppen–Geiger climate classification. *Hydrol. Earth Syst. Sci.*, **11**, 1633–1644, doi:10.5194/hessd-4-439-2007.

Qin, Z., A. Karnieli, and P. Berliner, 2001: A mono-window algorithm for retrieving land surface temperature from Landsat TM data and its application to the Israel–Egypt border region. *Int. J. Remote Sens.*, **22**, 3719–3746, doi:10.1080/01431160010006971.

Schatz, J., and C. J. Kucharik, 2014: Seasonality of the urban heat island effect in Madison, Wisconsin. *J. Appl. Meteor. Climatol.*, **53**, 2371–2386, doi:10.1175/JAMC-D-14-0107.1.

Scott, A. A., B. Zaitchik, D. Waugh, K. O'Meara, C. Hickman, and S. Stoerkel, 2016: Data associated with Scott et al 2016, intra-urban temperature variability in Baltimore, version 1. Johns Hopkins University Data Archive, accessed 1 July 2016, doi:10.7281/T10Z715B.

Smargiassi, A., M. S. Goldberg, C. Plante, M. Fournier, Y. Baudouin, and T. Kosatsky, 2009: Variation of daily warm season mortality as a function of micro-urban heat islands. *J. Epidemiol. Community Health*, **63**, 659–664, doi:10.1136/jech.2008.078147.

Smith, R. B., 2010: The heat budget of the earth's surface deduced from space. Yale University Center for Earth Observation Rep., 11 pp. [Available online at http://yceo.yale.edu/sites/default/files/files/Surface_Heat_Budget_From_Space.pdf.]

Smoliak, B. V., P. K. Snyder, T. E. Twine, P. M. Mykleby, and W. F. Hertel, 2015: Dense network observations of the Twin Cities canopy-layer urban heat island. *J. Appl. Meteor. Climatol.*, **54**, 1899–1917, doi:10.1175/JAMC-D-14-0239.1.

Stewart, I. D., and T. R. Oke, 2012: Local climate zones for urban temperature studies. *Bull. Amer. Meteor. Soc.*, **93**, 1879–1900, doi:10.1175/BAMS-D-11-00019.1.

Sun, Y.-J., J.-F. Wang, R.-H. Zhang, R. R. Gillies, Y. Xue, and Y.-C. Bo, 2005: Air temperature retrieval from remote sensing data based on thermodynamics. *Theor. Appl. Climatol.*, **80**, 37–48, doi:10.1007/s00704-004-0079-y.

Voogt, J. A., and T. R. Oke, 2003: Thermal remote sensing of urban climates. *Remote Sens. Environ.*, **86**, 370–384, doi:10.1016/S0034-4257(03)00079-8.

White-Newsome, J. L., S. J. Brines, D. G. Brown, J. T. Dvonch, C. J. Gronlund, K. Zhang, E. M. Oswald, and M. S. O'Neill, 2013: Validating satellite-derived land surface temperature with in situ measurements: A public health perspective. *Environ. Health Perspect.*, **121**, 925–931, doi:10.1289/ehp.1206176.

WMO, 2010: WMO guide to meteorological instruments and methods of observation. World Meteorological Organization Rep. WMO-8, 715 pp. [Available online at http://library.wmo.int/pmb_ged/wmo_8_en-2012.pdf.]

——, 2014: Atlas of mortality and economic losses from weather, climate and water extremes (1970–2012). World Meteorological Organization Rep. WMO-1123, 44 pp. [Available online at http://public.wmo.int/en/resources/library/atlas-mortality-and-economic-losses-weather-and-climate-extremes-1970-2012.]

Xu, Y., and Y. Liu, 2015: Monitoring the near-surface urban heat island in Beijing, China by satellite remote sensing. *Geogr. Res.*, **53**, 16–25, doi:10.1111/1745-5871.12092.

Zaitchik, B. F., K. O'Meara, K. Baja, A. A. Scott, D. W. Waugh, and M. C. McCormack, 2016: B'more cool: Monitoring the urban heat island at high density for health and urban design. *Earthzine*, 23 February 2016. [Available online at https://earthzine.org/2016/02/23/bmore-cool-monitoring-the-urban-heat-island-at-high-density-for-health-and-urban-design/.]

Zhao, L., X. Lee, R. B. Smith, and K. Oleson, 2014: Strong contributions of local background climate to urban heat islands. *Nature*, **511**, 216–219, doi:10.1038/nature13462.